

國立交通大學

電信工程研究所

碩士論文

毫微微細胞覆蓋式正交分頻多工網路之分散式資源分配

Distributed Resource Allocation in an OFDMA-based Femtocell Overlay Network

研究生：黃泓錫

指導教授：蘇育德 博士

中華民國 一 百 年 十 一 月

毫微微細胞覆蓋式正交分頻多工
網路之分散式資源分配

Distributed Resource Allocation in an
OFDMA-based Femtocell Overlay Network

研究生：黃泓錫

Student : Hung-Hsi Huang

指導教授：蘇育德 博士

Advisor : Dr. Yu T. Su

國立交通大學
電信工程研究所
碩士論文

A Thesis

Submitted to Institute Communications Engineering

College of Electrical and Computer Engineering

National Chiao Tung University

in partial Fulfillment of the Requirements

for the Degree of

Master

in

Communications Engineering

November 2011

Hsinchu, Taiwan, Republic of China

中華民國一十年十一月

毫微微細胞覆蓋式正交分頻多工網路之分散式資源分配

研究生：黃泓錫

指導教授：蘇育德 博士

國立交通大學電信工程學系碩士班

中文摘要

毫微微蜂巢式網路(femtocell)具有延伸網路涵蓋範圍、提昇網路傳輸容量、增加服務品質等優勢，此外也可以補強大型基地台(macrocell)無法涵蓋的區域和死角，並減輕其頻寬負荷。即使毫微微蜂巢式網路有上述好處，為了保持大型網路使用者的傳輸品質，這些毫微微蜂巢式網路皆會有最大功率下載限制。

在此篇文章中使用閉路存取之正交分頻多工存取(OFDMA)蜂巢網路，並深入探討如何提升通道傳輸容量以及干擾控制。我們使用中斷機制來量測大型網路使用者的訊號品質，除此之外我們也採用有干擾限制下之分散式迭代法來處理資源分配。中斷機率的運算可以讓毫微微蜂巢式網路基地台不需要知道大型網路使用者的確切位置、通道上的訊號以及受到的干擾。但每個毫微微蜂巢式網路基地台使用分散式方法計算通道傳輸容量時，則需要知其覆蓋範圍底下使用者通道狀況或是訊號干擾雜訊比。

毫微微蜂巢式網路基地台在分散式資源分配演算法裡的每一回合，會根據網路內使用者在頻帶上的通道狀態以及訊號干擾雜訊比，將頻帶適當的分配給其下之使用者，再使用注水演算法來分配所有頻帶上的功率。透過平均中斷機率的要求，每個頻帶上皆會有最大的功率限制。我們因此提出修正式注水演算法程序來最大化每個毫微微蜂巢式網路傳輸容量。當我

們觀察到所提出的方法不一定都會收斂，因此我們再提出多個修正措施來增加收斂的機率。分散式資源分配也可以視為某種非合作式賽局，透過已知奈許平衡點之充分條件，試著將其與我們所提出的演算法和修正措施之收斂性做一個結合。



Distributed Resource Allocation in an OFDMA-based Femtocell Overlay Network

Student : Hung-Hsi Huang Advisor : Yu T. Su

Communications Engineering
National Chiao Tung University

Abstract

The deployment of femtocells is an attractive solution to cope with the capacity and coverage limitation of the existing macrocellular networks. For femtocells to overlay an existing macrocellular network, it is important that the signal qualities of macrocell users (mMSs) be maintained, i.e., the femto-users induced interference be limited to a tolerable level.

In this thesis, we discuss the capacity enhancement and interference control issues in a closed access two-tier orthogonal frequency division multiple access (OFDMA) based cellular network. We use the average outage probability as the measure of mMS signal quality and employ an iterative distributed resource allocation (RA) based interference control approach. The former measure avoids the need for a femto base station (fBS) to know the exact locations of mMSs and the related signal and interference link gains while the distributed approach assumes that each fBS has access to the link gains or signal to noise-plus-interference ratio (SINR) associated with all downlinks within its coverage only.

At each iteration of the distributed RA algorithm, each fBS selects a femto mobile station (fMS) for every subcarrier according to the link gain and SINR and uses a water-filling procedure for power allocation. The average outage probability requirement,

however, impose a peak power constraint on each subcarrier. We thus suggest a modified water-filling procedure to maximize the sum capacity of a femtocell. As we observe that the proposed method does not necessarily converge, we propose several remedies to improve the convergence probability. Regarding the distributed RA as a noncooperative game and use a known sufficient condition for the existence of a Nash equilibrium point, we try to interpret the convergence behavior of our algorithm and its remedies.



誌 謝

首先要感謝指導教授 蘇育德博士，老師除了在研究上諄諄教誨，做人處事態度也令我受益匪淺。另外也感謝口試委員吳文榕教授、楊谷章教授以及魏存毅教授給予寶貴意見，彌補此篇論文不足及缺失之處。實驗室方面，特別感謝劉彥成學長在論文方面大力指導，林坤昌學長及劉人仰學長指點迷津，以及張致遠學長在精神方面支持。也由衷感謝實驗室其他學長姐、同學以及學弟妹，在生活上的幫忙以及鼓勵。

最後，感謝我最深愛的家人，能在這一路上不斷支持我，他們的關心與鼓勵帶给了我無形的動力，僅獻上此論文，以代表我最深的敬意。

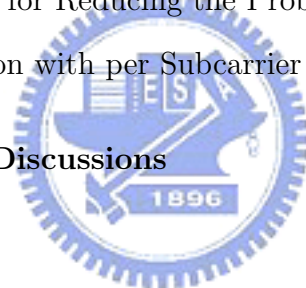


Contents

Chinese Abstract	i
Chinese Abstract	ii
English Abstract	iii
Acknowledgements	v
Contents	vi
List of Figures	viii
List of Tables	x
1 Introduction	1
2 Scenario and Assumption	6
3 Outage Probability Constraint	10
3.1 Distributed Locations of fBSs	13
3.2 fBSs Fixed in Femtoblock	14
3.3 Simulated Outage Probabilities	15
4 Noncooperative Game	19
4.1 Noncooperative Game	19
4.2 Non-cooperative Resource Allocation Game	20



4.2.1	Nash Equilibrium	21
4.2.2	Algorithm of Noncooperative Game	21
4.2.3	Algorithm of Subcarrier Assignment	22
4.2.4	Noncooperative Power Allocation Game	23
4.2.5	Randomization	24
	▶ Scheme 1	24
	▶ Scheme 2	24
5	Convergence and Unique NE point	25
5.1	Sufficient Condition for Unique NE Point	25
5.2	Non-Convergence of Distributed Approach	27
	5.2.1 Causes and Cases of Oscillation	27
	5.2.2 Randomization for Reducing the Probability of Oscillation	29
	5.2.3 Power Allocation with per Subcarrier Power Constraint	29
6	Numerical Results and Discussions	34
7	Conclusion	41
	Bibliography	43
	Vita	44



List of Figures

1.1	Typical femtocell deployment scenario.	2
2.1	A two-tier OFDMA cellular network that consists of a mBS, multiple femto-blockS, mMSSs, fBSs, and fMSs.	7
2.2	A femtocell block.	7
2.3	Interference between different femtocells.	8
3.1	Outage probability under different power upper bound.	15
3.2	Outage probability under different power upper bound with distance between mBS and femtoblock=50.	16
3.3	Outage probability under different power upper bound with distance between mBS and femtoblock=300.	16
3.4	Outage probability under different power upper bound with distance between mBS and femtoblock=700.	17
3.5	Outage probability under different power upper bound with distance between mBS and femtoblock=1500.	17
5.1	Oscillation.	27
5.2	Randomization.	31
5.3	Illustration of water-filling interpretation with power upper bound.	32
5.4	Illustration of water-filling interpretation with power upper bound.	33
6.1	Convergence Case of Noncooperative Game.	35

6.2	Nonconvergence Case of Noncooperative Game.	36
6.3	Convergence result by using Variance Reduction	36
6.4	Iteration number with different power upper bound.	37
6.5	Iteration numbers versus probability of using randomization 1.	38
6.6	Iteration numbers versus probability of using randomization 2.	38
6.7	Comparison of Femtocell Capacity.	39
6.8	Femtocell capacity versus SIR constraints of mMS with different power constraints.	40



List of Tables

6.1 Simulation parameters. 34

6.2 Pathloss model. 35



Chapter 1

Introduction

In recent years, the demand for higher data rates in wireless networks is dramatically increased. Besides, extending coverage into residential areas is one of the biggest challenges for current mobile communication networks. Since it is extremely expensive to serve the indoor users with large service demands, a significant interest within the telecommunications industry has recently focused on how to provide service for indoor users in a cost-efficient way and femtocell is introduced to solve the cost and efficiency issues.

The femtocells use the same spectrum with macrocell and it enhances the indoor coverage of macrocell by deploying a low-power, low-cost, and short-range base station in indoor environment. Due to short distance between femtocell base station (fBS) and femtocell mobile users (fMSs), femtocell can achieve high throughput with low transmission power of femtocell. The fBSs can be installed by consumers themselves inside offices or houses. It connects to macrocell system via internet, such as Digital Subscriber Line (DSL), cable modem or fiber; the whole femtocell network scenario is illustrated in Fig. 1.1 [1]. Since femtocell is installed in indoor environment, it can provide high data rate for indoor users. Meanwhile, because macrocells only need to allocate resources to outdoor mobile users, the reliability of macrocell mobile users is enhanced.

The Orthogonal Frequency Division Multiple Access (OFDMA) has been widely

adopted or considered as a candidate of multiple access scheme for future wide area broadband wireless networks with its robustness against frequency selective fading and its flexibility in radio resource allocation for satisfying various QoS requirements. OFDMA exploits multi-user diversity in time-varying and frequency-selective fading channels by assigning a subcarrier to the user with the best channel gain and by scheduling the transmission of user data opportunistically.

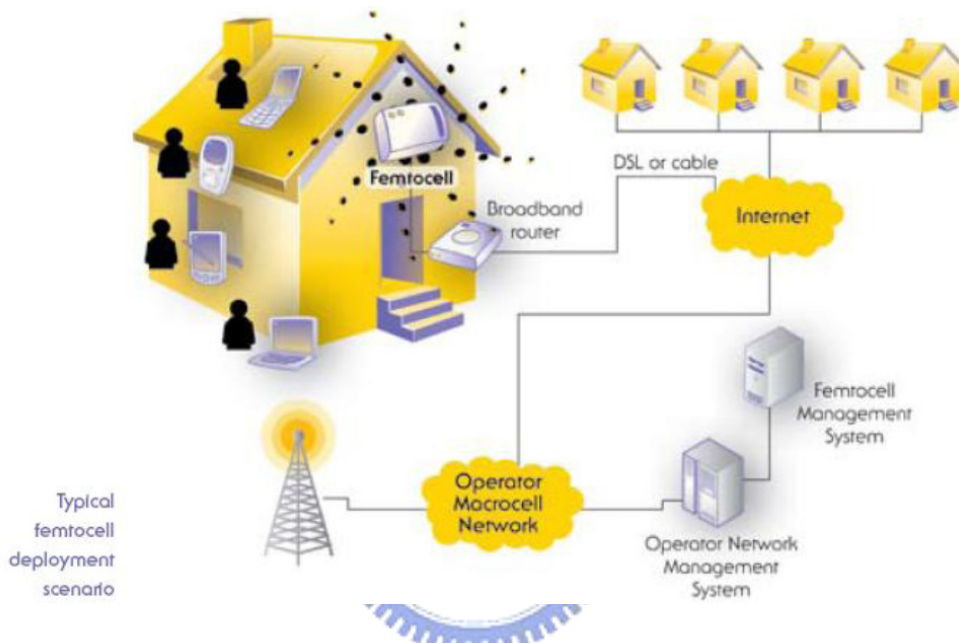


Figure 1.1: Typical femtocell deployment scenario.

However, some technical challenges must be discussed concerning femtocell network. For instance, timing and synchronization, cross-tier interference avoidance, access method of femtocell, and handover between macrocell and femtocell, those issues are critical aspects of femtocell technology which still need be studied further. In addition, for the coexistence scheme, the overall capacity may be reduced significantly due to the co-channel interference. Therefore, how to deal with the interference management is also an important issue concerning femtocell networks and it is studied in this thesis.

A hybrid spectrum sharing scheme is also proposed to reduce interference in [2]. In [3], spectrum sensing and subchannel assignment are joint considered to reduce intercell

interference and to increase system capacity in the meanwhile. [4] considered a optimization problem maximizing femtocell network capacity with constraints restricting femtocell power such that the communication between macro BS and outdoor users is not interrupted. Chandrasekhar develops interference avoidance strategy in a two-tier Code Division Multiple Access (CDMA) network in [5] and Spatial Poisson Point Process (SPPP) [6] is utilized to model distribution of femtocell base stations.

Nevertheless, assuming the perfect information about the channel and/or location of may not be true in practice. To deal with this issue, we propose average outage probability constraint to restrict interference caused by femtocell without the perfect assumption. We define that outage event occurs when received SIR of macrocell users below a predefined threshold, and we control femtocell such that the outage probability is lower than the predetermined tolerance threshold. As we known, the outage probability is widely utilized to represent the coverage of a broadcast network. The coverage is based on the outage probability that the carrier-to-noise ratio (CNR) of a received signal at any location within its coverage area is greater than a predetermined threshold [7]. Based on the average outage probability constraint, we transform the average outage probability constrain into the maximum transmission power constraint easily.

After finding the maximum tolerant transmission power of femtocell according average outage probability constraint, we want to solve the resource allocation problem of femtocell system. In this thesis, the femtocells are secondary users that coexist with primary users that are macro users. The macro users are licensed to operate over certain frequency bands. They do not cooperate with or even provide feedback to the fBSs. One of the main challenges in femtocells is how to design an efficient and adaptive channel access scheme that supports dynamic subcarrier selection and power/rate allocation in a distributed femtocell environment. Here, we want to use game theory to formulate the resource allocation game of our system.

Several attempts with game theory have been made to solve the resource allocation

problem. In [8], the noncooperative game is used to deal with the resource allocation problems. However, the proof of the noncooperative game does not consider the subcarrier allocation and the standard function seems inappropriate to prove the convergence of the game. Besides, the authors do not discuss the power upper bound for the system to protect the primary users' rights. In [9], though the authors claim that their noncooperative game can converge if the subcarrier allocation is stable, they do not prove the game can converge to a unique NE point. In [10], the sufficient condition of unique NE point is provided and the algorithm can converge to a NE point under some conditions. However, the authors do not discuss the user selection and only focus on the power allocation.

In [11], the authors use noncooperative pricing game and also claim their game can converge to a Pareto-optimum solution. However, this game needs to use MAC layer to communicate the signals between different users that takes too much time and overhead to communicate each other. A centralized spectrum management scheme was proposed in [12], which greatly improves the system performance over the IWF scheme by utilizing a centralized spectrum management center (SMC). However, such an approach cannot be implemented in an ad hoc opportunistic cognitive radio network (CRN), where none of the cognitive radios has global knowledge of the entire CRN to function as the SMC.

Given the above, we are motivated to design a channel/power/rate allocation scheme that can solve the resource allocation problem and can be implemented in a distributed fashion. We provide a noncooperative game that consider not only power allocation but also user selection. Besides, we discuss the sufficient condition of converging to a unique NE point in our noncooperative game. On the other hand, our distributed algorithm can also reduce the non-convergence probability of resource allocation. We also compare the bandwidth efficiency of distributed algorithm with centralized approach. Finally, the simulation of bandwidth efficiency for femtocell system with power upper bound in a practical system is illustrated.

The rest of this thesis is organized as follows. In following chapter, we present the scenario and assumption of our system model. The outage probability is provided to satisfy the rights of macrocell in chapter 3. In chapter 4, we proposed a noncooperative game and algorithm to solve the resource allocation problem. We investigate the non-convergence cases and prove that our algorithm definitely reduces the probability of non-convergence in chapter 5. Finally, chapter 6 represents some simulation results and this thesis ends up with some conclusions in chapter 7.



Chapter 2

Scenario and Assumption

The network layout under investigation is illustrated in Fig. 2.1. An overlay system consists of a macro base station (mBS) at the center of the macrocell and J macro users randomly located in the macrocell is depicted. Without loss of generality, we only need to consider one third sector of a macrocell. We assume a femtoblock, containing K femtocells, is randomly located in the macrocell. There are L_k ($k = 1, 2, \dots, K$) femtocell users (fMSs) randomly distributed in the femtocell k . The total bandwidth of the system is equally divided into N OFDM subcarriers.

In Fig. 2.2, a dense-urban femtocell model, each block represents two stripes of apartments and each stripe has $2N$ apartments. Each apartment is of size $10\text{m} \times 10\text{m}$. There is a street between the two stripes of apartments, with width of 10m . Each femtocell block is of size $10(N+2)\text{m} \times 70\text{m}$. In each macrocell sector, one or several femtocell blocks may exist while it is assumed that the femtocell blocks are not overlapping with each other.

While a centralized algorithm can solve our problem effectively, its requirement that the centralized controller needs to know all information about all subcarriers and of high computational complexity to optimize jointly makes it difficult to implement in a practical system. Thus, we consider a more pragmatic system where each fBS only knows its total transmit power P_{fem} , channel gain to its own fMSs, and the interference

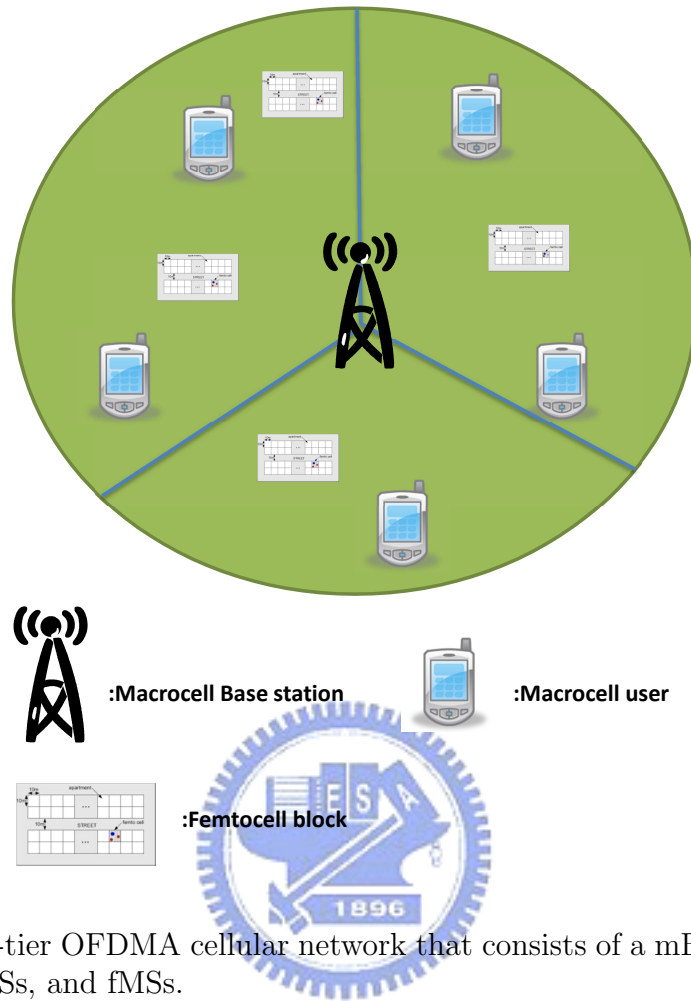


Figure 2.1: A two-tier OFDMA cellular network that consists of a mBS, multiple femto-blockS, mMSs, fBSs, and fMSs.

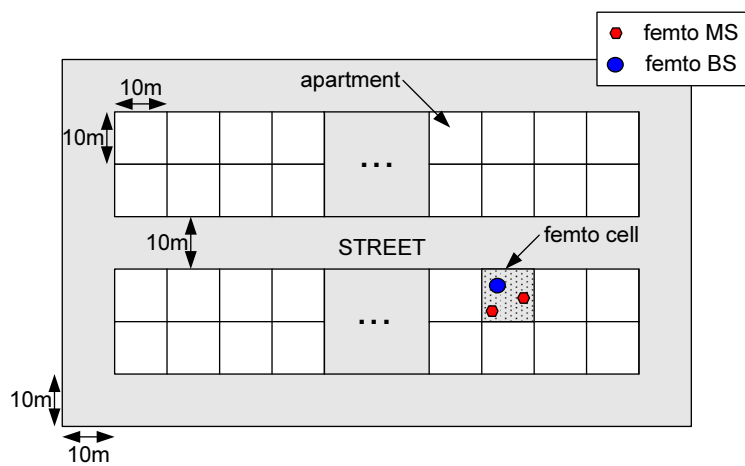


Figure 2.2: A femtocell block.

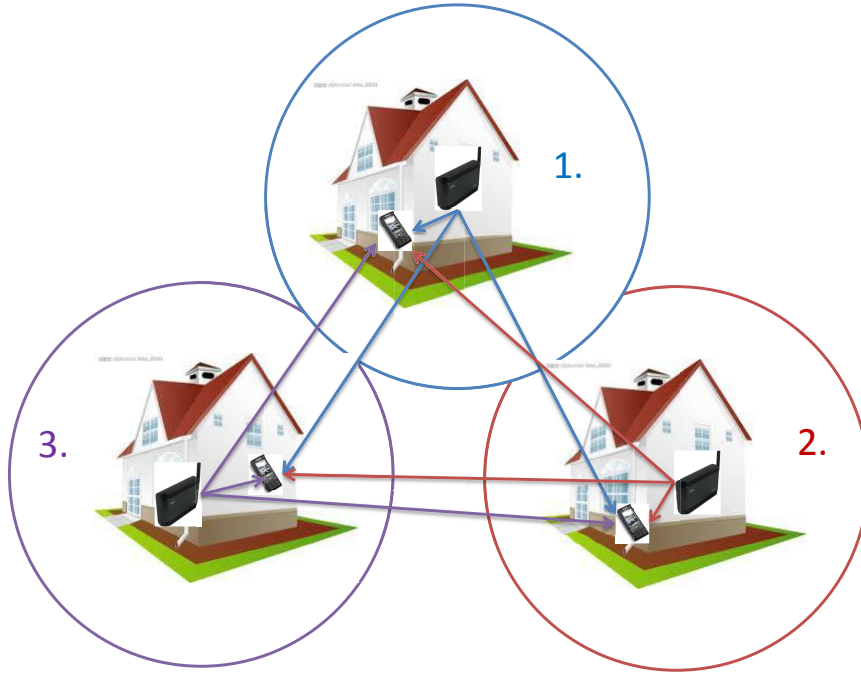


Figure 2.3: Interference between different femtocells.

from other fBSs and mBS to their fMSs. However, if each fBS aims to maximize its own achievable rate with its fMSs selfishly without cooperating with other fBSs, it may causes severe interference to the nearby femtocells. Thus, every fBS needs to not only maximize its sum rates but also adapts to other fBSs' interference. A simplified example is illustrated in Fig 2.3.

We denote by $\mathbf{p}_k = [p_k^1, p_k^2, \dots, p_k^N]$ the **transmission power vector** of fBS k , where p_k^n is the transmission power on subcarrier n of fBS k . In addition, we denote by $\mathbf{p} = [\mathbf{p}_1, \mathbf{p}_2, \dots, \mathbf{p}_K]$ the **network power vector**. We restrict the total transmission power (i.e., $\sum_{n=1}^N p_k^n$) of each fBS k to be no more than P_{fem} . We define $\mathbf{A}_k = [a_{l,k}^n]_{l_k \times N}$ as the **assignment matrix**, where $a_{l,k}^n$ is 1 if the subcarrier n is assigned to user l and 0 otherwise and each subcarrier can be assigned to no more than one fMS in each femtocell.

We let the channel gain containing path loss and independent fading from fBS i to fMs l in femtocell k on subcarrier n be represented by $h_{il,k}^n$ and the transmit power

from fBS i to fMs l in femtocell k on subcarrier n by $p_{il,k}^n$. Their mBS counterparts are denoted by $h_{ml,k}^n$ and $p_{ml,k}^n$ by substituting subscript i by m .

The total interference received by fMs l in femtocell k on subcarrier n is denoted by $I_{l,k}^n$ which consists of the interference from mBS $p_{ml,k}^n h_{ml,k}^n$ and the aggregated interference from other fBSs except fBS k $\sum_{i=1, i \neq k}^K p_{il,k}^n h_{il,k}^n$. Without loss of generality, the noise power σ^2 on all subcarriers are assumed to be the same. We define the gain-to-noise-plus-interference ratio (GINR) of fMS l in femtocell k on subcarrier n as

$$g_{l,k}^n = \frac{h_{kl,k}^n}{I_{l,k}^n + \sigma^2} = \frac{h_{kl,k}^n}{p_{ml,k}^n h_{ml,k}^n + \sum_{i=1, i \neq k}^K p_{il,k}^n h_{il,k}^n + \sigma^2} \quad (2.1)$$

The sum rate of fMS l in femtocell k is thus

$$\sum_{n=1}^N a_{l,k}^n \log_2(1 + p_{kl,k}^n g_{l,k}^n). \quad (2.2)$$



Chapter 3

Outage Probability Constraint

The motivation of using femtocell system is to enhance the spectrum utilization by allowing femtocell base stations (fBSs) to share the same spectrum with the macrocell system. While in our overlay downlink system, because fBSs only serve their femtocell users (fMSs) in its serving area, the signal of a fBS is interference to nearby users as mMSs and fMSs in other femtocells.

Since in our overlay system the mMSs are the primary users, fBSs cannot cause too large interference and damage the QoS of their nearby mMSs. Due to the randomness of the mMS locations, it is impractical to assume perfect knowledge of mMS location at a fBS. Besides, the fBSs are installed by consumers; the fBSs do not have the information about the macrocell network, such as the channel state information (CSI) between the mBS and mMSs and the information about the frequency assignments of macrocell network. Therefore, the exact calculation of the interference caused by fBSs to mMSs is difficult. We will illustrate how those fBSs allocate their resource to avoid causing too much interference to their nearby mMSs as well as maintain the mMSs' QoS.

In this Chapter, the average outage probability constraint for protecting the mMSs' QoS is discussed. An outage event occurs when the received signal-to-interference-ratio (SIR) of a mMS on a subcarrier n γ_n is smaller than or equal to a the predefined threshold η_n . Then, the corresponding outage probability P_o can be expressed as

$$P_o = P_r\{\gamma_n \leq \eta_n\}. \quad (3.1)$$

The setting of SIR threshold η_n depends on the application and priority of the mMBS. If the received SIR is higher than η_n , the mMBS can decode the data correctly. Otherwise, the mMBS cannot have reliable data. The notion of outage probability constraint means that the outage probability is restricted not to exceed a specified threshold P_{out} .

If we limit the outage probability to be less than or equal to the predefined threshold P_{out} , the interference will also be restricted; therefore, the QoS of macrocell can be guaranteed. The determination of outage probability threshold P_{out} also depends on the application of the communication link and the priority of the mMBS. In general, the higher the QoS is required, the lower the threshold should be.

As a result, the outage probability constraint provides another dimension to adjust the behavior of fBS. Specifically, as the threshold P_{out} may vary across different subcarriers, a fBS can adjust its power allocation and/or subcarrier assignment based on these different outage probability constraints. Therefore, by limiting the possibility of the outage probabilities, we also limit the amount of interference such that QoS of mMBSs is satisfied.

Since the fBS does not have the exact instantaneous information of macrocell (e.g., CSI between mBS and mMBSs and the exact locations of mMBSs), we need to average out all unknown information of mMBSs. Given the fixed locations of mMBSs and all fBSs, we average out the channel gain between all fBSs and mMBSs and that between a mBS and its mMBSs. The closed form of the outage probability conditioned on the fixed locations is first derived. Then we average over different locations of fBSs and mMBSs to derive the average outage probability of mMBS. With the outage probability, we can find the power upper bound of all fBSs to satisfy the mMBSs' QoS.

While the distance between fBSs and mMBSs are determined once the consumer installed them, the mMBSs and fBSs are assumed uniformly located in the coverage region of a mBS. The distance between the mBS and the k th fBS is denoted by $r_{k,m}$ and the distance between the mBS and the j th mMBS is denoted by $r_{j,m}$. It is useful to for-

mulate the pdf of the distance $r_{j,m}$ and $r_{k,m}$ in polar coordinate system, which can be represented as

$$f_{r_{j,m}}(r) = \frac{2r}{R_{max}^2 - R_{min,j}^2} \quad (3.2)$$

$$f_{r_{k,m}}(r) = \frac{2r}{R_{max}^2 - R_{min,k}^2} \quad (3.3)$$

where r is the distance measured from mBS. The parameters R_{max} is the maximum radius of macrocell, and $R_{min,j}$ ($R_{min,k}$) is the minimum distance between the j th mBS and the k th mMMS (fBS). For convenience, we assume that $R_{min,m}=R_{min,k}=R_{min}$. Moreover, we can express the distance between the j th mMMS and the k th fBS by law of cosines:

$$r_{j,k} = \sqrt{r_{j,m}^2 + r_{k,m}^2 - 2r_{j,m}r_{k,m} \cos \theta_{j,k}} \quad (3.4)$$

where $\theta_{j,k}$ is the angle between the line connecting mBS and j th mMMS and that connecting mBS and the k th fBS.

Recall that the macrocell is a 3-sector system. Since the mMMSs and fBSs are uniformly random located in the sectorized region, the random variable $\theta_{j,k}$ is assumed to conform a uniform random variable with domain $[0, \frac{2\pi}{3}]$.

The distribution of $r_{j,k}$ thus depends on three independent random variables $r_{j,m}$, $r_{k,m}$, and $\theta_{j,k}$. However, direct deriving the exact pdf of $r_{j,k}$ is rather difficult, we will approximate the outage probability P_o via Monte Carlo method. While P_o is obtained by 10^6 realizations of $r_{j,m}$, $r_{k,m}$ and $\theta_{j,k}$, in the next section we will keep the expression of $f_{r_{j,k}}$, the pdf of $r_{j,k}$.

We first derive the closed form of the outage probability conditioned on fixed locations of fBSs and mMMSs. Then, we average over possible locations of all mMMSs and fBSs to find the average outage probability. We examine two different scenarios: one where each fBS is independent randomly distributed in the macrocell; the other all fBSs gather together in a femto-block which is randomly distributed in the macrocell.

3.1 Distributed Locations of fBSs

We first fix the locations of mMSSs and fBSs and find the outage probability $P_{o,fix}$ conditioned on these locations.

$$P_{o,fix} = P_r \left\{ \frac{p_{mj,m}^n h_{mj,m}^n}{\sum_{k=1}^K p_{kl,k}^n h_{kj,m}^n} \leq \eta_n |r_{j,m}, r_{j,1}, r_{j,2} \dots r_{j,K} \right\} \quad (3.5)$$

$$= P_r \left\{ \frac{p_{mj,m}^n |H_{mj,m}^n|^2 PL(r_{j,m})}{\sum_{k=1}^K p_{kl,k}^n |H_{kj,m}^n|^2 PL(r_{j,k})} \leq \eta_n |r_{j,m}, r_{j,1}, r_{j,2} \dots r_{j,K} \right\} \quad (3.6)$$

$$= P_r \left\{ \frac{\sum_{k=1}^K p_{kl,k}^n |H_{kj,m}^n|^2 PL(r_{j,k})}{p_{mj,m}^n |H_{mj,m}^n|^2 PL(r_{j,m})} \geq \frac{1}{\eta_n} |r_{j,m}, r_{j,1}, r_{j,2} \dots r_{j,K} \right\}$$

$$= P_r \left\{ \sum_{k=1}^K p_{kl,k}^n |H_{kj,m}^n|^2 PL(r_{j,k}) \geq \gamma p_{mj,m}^n |H_{mj,m}^n|^2 PL(r_{j,m}) |r_{j,m}, r_{j,1}, r_{j,2} \dots r_{j,K} \right\}$$

$$= P_r \left\{ \sum_{k=1}^K W_k |H_{kj,m}^n|^2 \geq \gamma W_m |H_{mj,m}^n|^2 |r_{j,m}, r_{j,1}, r_{j,2} \dots r_{j,K} \right\} \quad (3.7)$$

$$= P_r \left\{ z \geq \gamma W_m |H_{mj,m}^n|^2 |r_{j,m}, r_{j,1}, r_{j,2} \dots r_{j,K} \right\} \quad (3.8)$$

$$\begin{aligned} &= \int_0^\infty \int_{\gamma W_m |H_{mj,m}^n|^2}^\infty \sum_{k=1}^K \frac{C_k}{W_k} \exp\left(-\frac{z}{W_k}\right) dz \exp(-|H_{mj,m}^n|^2) d|H_{mj,m}^n|^2 \\ &= \sum_{k=1}^K \int_0^\infty \int_{\gamma W_m |H_{mj,m}^n|^2}^\infty \frac{C_k}{W_k} \exp\left(-\frac{z}{W_k}\right) dz \exp(-|H_{mj,m}^n|^2) d|H_{mj,m}^n|^2 \\ &= \sum_{k=1}^K \int_0^\infty C_k \exp\left(-\frac{\gamma W_m |H_{mj,m}^n|^2}{W_k}\right) \exp(-|H_{mj,m}^n|^2) d|H_{mj,m}^n|^2 \\ &= \sum_{k=1}^K \frac{C_k W_k}{\gamma W_m + W_k} \end{aligned} \quad (3.9)$$

Where $h_{mj,m}^n$ and $h_{kj,m}^n$ contains the fading gain and path loss, $\gamma = \frac{1}{\eta_n}$, $W_k = p_{kl,k}^n PL(r_{j,k})$ and $W_m = p_{mj,m}^n PL(r_{j,m})$. In (3.8), we have let $z = \sum_{k=1}^K W_k |H_{kj,m}^n|^2$, a weighted sum of exponentially distributed random variables, with pdf being $\sum_{k=1}^K \frac{C_k}{W_k} \exp\left(-\frac{z}{W_k}\right)$, where $C_k = \prod_{i=1, i \neq k}^K \frac{1}{1 - \frac{W_i}{W_k}}$ [13].

Because fBSs' and mMSSs' locations are randomly distributed in the macrocell, the

outage probability P_o is derived by average:

$$P_o = P_r\{\gamma_n \leq \eta_n\} \quad (3.10)$$

$$= E_{r_{j,m}, r_{j,1}, \dots, r_{j,K}} \left[\sum_{k=1}^K \frac{C_k W_k}{\gamma W_m + W_k} \right] \quad (3.11)$$

$$= \int \dots \int \int \sum_{k=1}^K \frac{C_k W_k}{\gamma W_m + W_k} f_{r_{j,m}}(r_o) f_{r_{j,1}}(r_1), \dots, f_{r_{j,K}}(r_K) dr_o dr_1, \dots, dr_K \quad (3.12)$$

3.2 fBSs Fixed in Femtoblock

Here, we discuss the case where K fBSs gather together in a femtoblock. In this accumulative scenario, all femtocells are located as illustrated in Fig. 2.2. Similarly,

$$P_{o,fix} = P_r\left\{ \frac{p_{mj,m}^n h_{mj,m}^n}{\sum_{k=1}^K p_{kl,k}^n h_{kj,m}^n} \leq \eta_n \right\} \quad (3.13)$$

$$= P_r\left\{ \frac{p_{mj,m}^n |H_{mj,m}^n|^2 PL(r_{mj,m})^*}{\sum_{k=1}^K p_{kl,k}^n |H_{kj,m}^n|^2 PL(r_{kj,m})^*} \leq \eta_n \right\} \quad (3.14)$$

$$= \sum_{k=1}^K \frac{C_k^* W_k^*}{\gamma W_m^* + W_k^*} \quad (3.15)$$

Note that the signal of all fBSs may penetrate more than one wall to reach mMSSs. Here we use super script \star to represent the path loss containing the penetration reflecting this effect.

Because K fBSs gather in a femtoblock, we may assume the distance between each fBS and mMSSs are the same when K is not too large. However, the numbers of walls between each fBS and mMSSs may differ according to their locations thus affecting W_k^* 's. Therefore, in this scenario, the outage probability can be approximated as

$$P_o = P_r\{\gamma_n \leq \eta_n\} \quad (3.16)$$

$$\approx \int \int \sum_{k=1}^K \frac{C_k^* W_k^*}{\gamma W_m^* + W_k^*} f_{r_{j,m}}(r_o) f_{r_{j,k}}(r_k) dr_o dr_k \quad (3.17)$$

We have formulated two closed forms of outage probability with fixed locations of mMSSs and fBSs. Thus the power upper bound of each fBS with different scenarios can

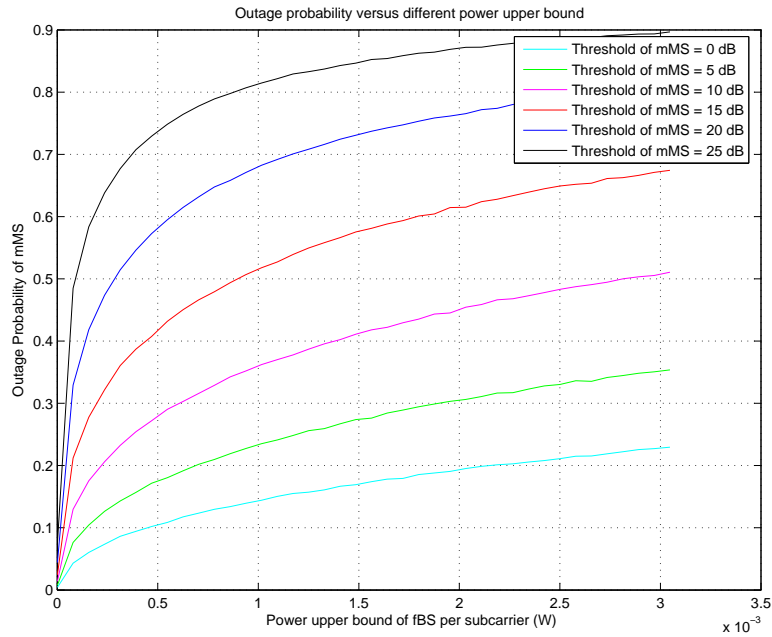


Figure 3.1: Outage probability under different power upper bound.

be obtained by averaging all possible locations produced by Monte Carlo method. The simulation results with two different scenarios in the next section.

3.3 Simulated Outage Probabilities

The outage probability we can tolerate in our system is 5% that means we only let 5% mMSs suffer severe interference and need to protect 95% mMSs' QoS. The BER we can accept in our fading channel system with channel coding is assumed 10^{-2} that means the SIR threshold of mMSs needs more than 10 dB. The outage probability of distributed locations of fBSs is shown in Fig. 3.1, we can find that as the QoS of mMSs increases, the mMSs restrict the maximum power fBSs can transmit. Thus the outage probability increases as the transmit power of fBSs increases. Besides, different SIR thresholds of mMSs also result in different outage probability.

There are another four simulation results with different distance between femtoblock

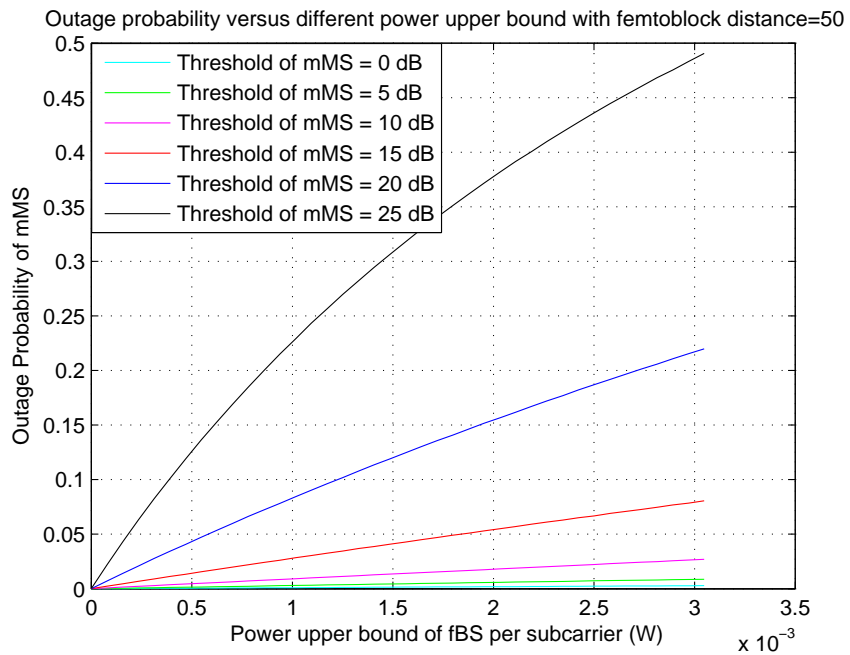


Figure 3.2: Outage probability under different power upper bound with distance between mBS and femtoblock=50.

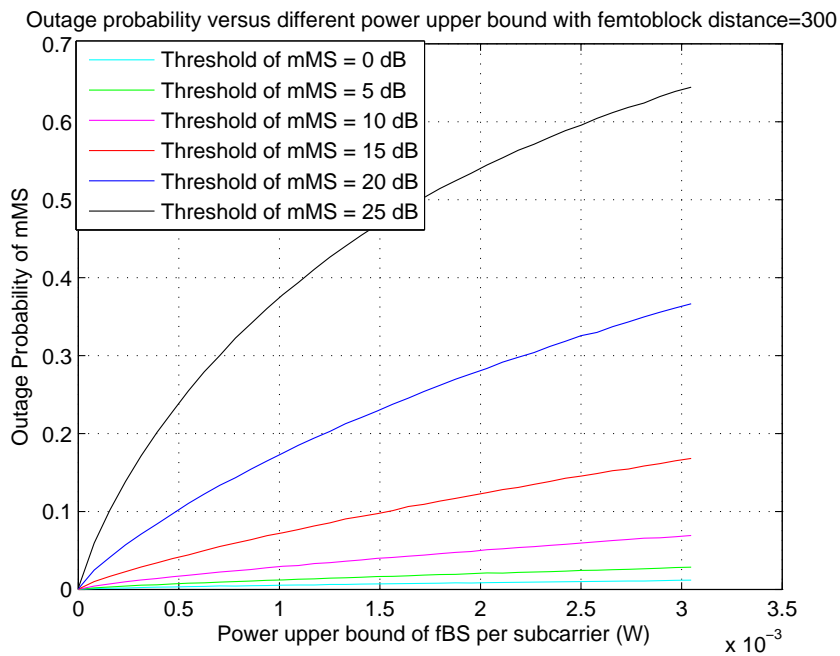


Figure 3.3: Outage probability under different power upper bound with distance between mBS and femtoblock=300.

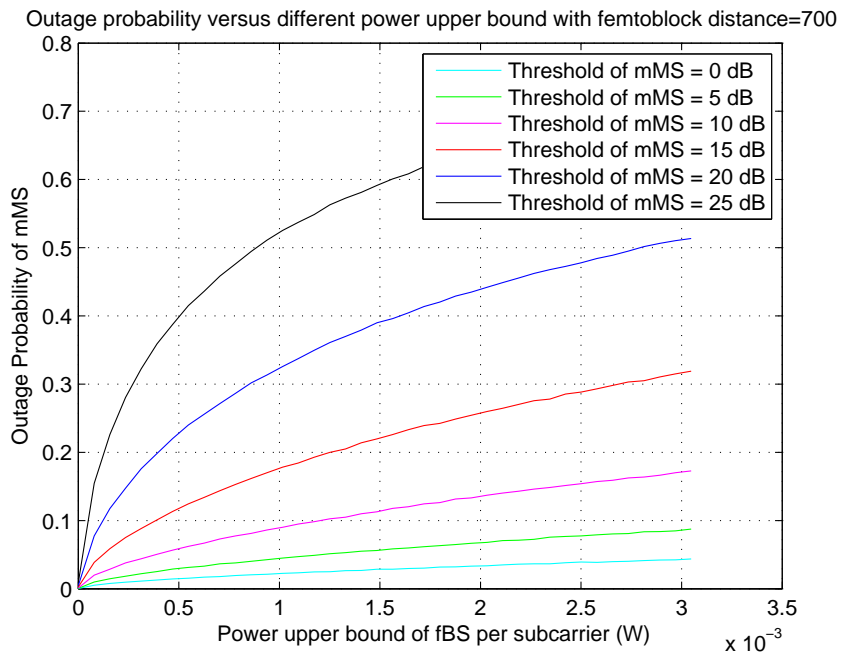


Figure 3.4: Outage probability under different power upper bound with distance between mBS and femtoblock=700.

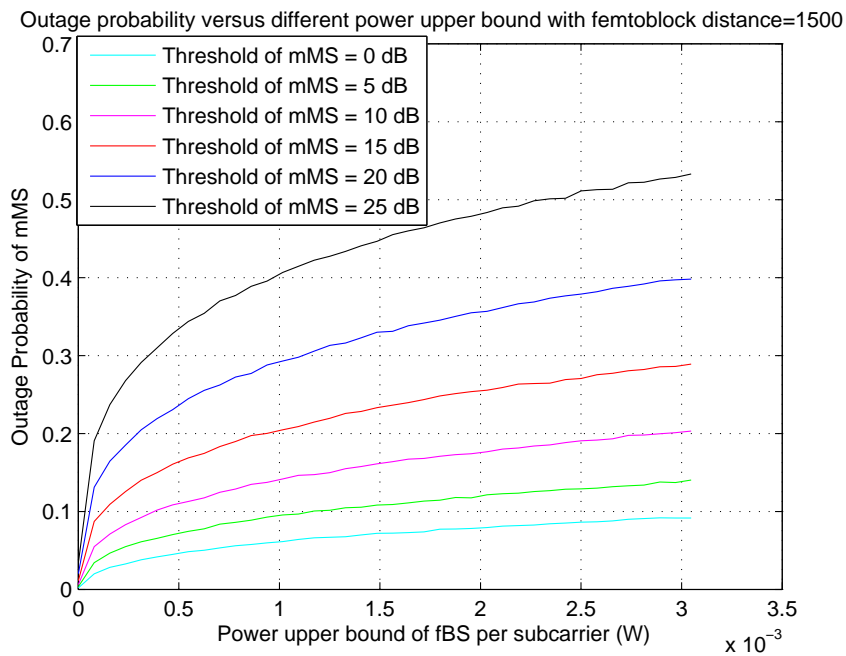


Figure 3.5: Outage probability under different power upper bound with distance between mBS and femtoblock=1500.

and mBS from Fig. 3.2–3.5. We can find as the requirements of mMSSs' SIR threshold increase, the outage probability of mMSSs also increases. The more power fBSs can transmit, the higher outage probability mMSSs achieve.

These four simulations also imply a fact that the outage probability has relation with the ratio of the distance between mBS and mMSS to the distance between fBS and mMSS that should be limited within a threshold r_{th} mainly dominated by the transmit power of mBS and fBSs, numbers of fBS, penetration loss and SIR requirement of mMSSs. Thus, when the distance between fBS and mMSS is 50m in Fig 3.2, the ratio of the distance between mBS and mMSS to the distance between fBS and mMSS is usually smaller than r_{th} , so the outage probability is low.

However, the distance between femto block and mBS is 700m in Fig. 3.4, the probability of the ratio of the distance that cannot satisfy the r_{th} increases, so the outage probability increases obviously. When fBSs are moved to location where the distance between mBS and fBSs is 1500 in Fig. 3.5, the outage probability with SIR threshold above 20dB is smaller than that in Fig. 3.4. The reason is that the outer part of the 1500m is limited by the convergence of mBS and the outer part of location at 700m from mBS is more than that of location at 1500m.

Chapter 4

Noncooperative Game

In this chapter, “game theory” is introduced to solve our resource allocation problem distributedly. Game theory is a tool to observe the interactions of players in decision-making processes, and provides some characteristics to be analyzed. The greedy behavior inherited in our sum-rate maximization problem and the interactions of femtocells in decision-making processes of resource allocation can be modeled and analyzed using game theory.

4.1 Noncooperative Game

We model the self-organized resource allocation as a non-cooperative game. In general, the noncooperative game consists of three components: players, strategies, and utilities, which can be mathematically defined as $G = \{\mathcal{K}, \{S_k\}_{k \in \mathcal{K}}, \{u_k\}_{k \in \mathcal{K}}\}$. The set of players and the set of strategies associated with player k are denoted as \mathcal{K} and S_k , respectively. The utility function of player k , $u_k: S \rightarrow \mathbb{R}$, maps each possible combination of the strategies of all players $S = S_1 \times S_2 \times \cdots \times S_k$, $k \in \mathcal{K}$, to a real value. The utility function represents the degree of satisfaction of player k as a function of the strategy it chooses, s_k , and the strategy of the other players, $s_{-k} = (s_1, \dots, s_{k-1}, s_{k+1}, \dots, s_K)$. The objective of each player is to choose the best strategy among the available strategies in order to maximize its own utility.

In our noncooperative game, the utility function should depend on the player k 's

action including power and subcarrier allocation and the union set of all other players' action \mathbf{p}_{-k} , where $\mathbf{p}_{-k} = [\mathbf{p}_1, \mathbf{p}_2, \dots, \mathbf{p}_{k-1}, \dots, \mathbf{p}_{k+1}, \dots, \mathbf{p}_K]$. Because our fBSs want to maximize their own sum capacity, the utility function of fBS k here is defined by $u_k(\mathbf{p}, A_k) = \sum_{l=1}^{L_k} \sum_{n=1}^N a_{l,k}^n \log_2(1 + p_{l,k}^n g_{l,k}^n)$.

Let $G = \{\mathcal{K}, \{\mathcal{P}_k \times \mathcal{A}_k\}, \{u_k\}\}$ denotes a **noncooperative resource allocation game** (NRAG), where $k \in \mathcal{K} = \{1, 2, \dots, K\}$ is the index set of the fBS. $\{\mathcal{P}_k \times \mathcal{A}_k\}$ is the strategy space of each fBS k with $\mathcal{P}_k = \{\mathbf{p}_k | 0 \leq \sum_{n=1}^N p_k^n \leq P_{fem}\}$ and $\mathcal{A}_k = \{\mathbf{A}_k | a_{l,k}^n \in \{0, 1\}, \sum_{l \in L_k} a_{l,k}^n = 1 \forall l, k\}$.

4.2 Non-cooperative Resource Allocation Game

For a specific femtocell k , it wants to maximize its utility function.

(p.1)

$$\max u_k(\mathbf{p}, A_k) = \sum_{l=1}^{L_k} \sum_{n=1}^N a_{l,k}^n \log_2(1 + p_{kl,k}^n g_{l,k}^n) \quad (4.1)$$

subject to

$$\sum_{l=1}^{L_k} \sum_{n=1}^N a_{l,k}^n p_{kl,k}^n \leq P_{fem} \quad (4.2)$$

$$p_{kl,k}^n \geq 0 \quad \forall l, n; \quad (4.3)$$

$$a_{l,k}^n \in \{0, 1\} \quad \forall l, n \quad (4.4)$$

$$\sum_{l=1}^{L_k} a_{l,k}^n \leq 1 \quad \forall n \quad (4.5)$$

$$p_{kl,k}^n \leq \bar{P}_{mac}^n \quad \forall l; \quad (4.6)$$

Equation (4.2) is the total power constraint of fBS k while the power constraints on each subcarrier are given in (4.3) and (4.6), where \bar{P}_{mac}^n obtained by outage probability in Chapter 3 represents the power upper bound on subcarrier n to satisfy the requirement of mM's QoS. The indicator constraints (4.4) and (4.5) are imposed to ensure that each subcarrier can be assigned to no more than one user.

The utility function of our noncooperative game is a non-convex problem and hard to solve, so we separate our problem into two parts: one is subcarrier allocation; the other power allocation. In the following sections, we will discuss the algorithm and the outcome of our game.

4.2.1 Nash Equilibrium

As the definition in the context of game theory, Nash equilibrium (NE) is a state where given other players' strategy, no player can improve its utility level by changing its own strategy unilaterally. If our noncooperative game can converge to a NE point, it means at this point no fBS wants to change its strategy of subcarrier and power allocation given other fBSs' strategies.

4.2.2 Algorithm of Noncooperative Game

Step 0: Initialize $t=0$ and T_{out} ;

Step 1: $t=t+1$;

Step 2: Each fMS measures the channel (GINR) for all the sub-channels and feeds back the measured values to the fBS.

Step 3: The fBS performs sub-channel assignment to the fMSs according to the algorithm of subcarrier assignment.

Step 4: The fBS performs power allocation according to the proposed power allocation method.

Step 5: (Oscillation monitoring) If the fBS observes there is oscillation on its subcarriers or power allocation compared to the previous stage, then it performs variation reduction.



Step 6: If the sum rate of each femtocell cannot achieve stable state, then go to step

1. If $t > T_{out}$ or sum rate of all fBSs become is stabilized, terminate.

Remark: (i) This algorithm is performed within each fBS. (ii) The convergence condition is that this fBS's capacity variation is less than 1%.

4.2.3 Algorithm of Subcarrier Assignment

Step 1: Initialize

$$a_{l,k}^n = 0, \forall k \in \{1, 2, \dots, K\}, \forall l \in \{1, 2, \dots, L_k\} \text{ and } \forall n \in \{1, 2, \dots, N\}$$

$$\text{and } S = \{1, 2, \dots, N\} \quad I_{l,k}^n(0) = 0$$

Step 2: for $k=1$ to K

while ($|S| \geq 1$)

$$l^*(n^*) = \arg \max_{l,n} g_{l,k}^n(t) = \arg \max_{l,n} \frac{h_{l,k}^n / \sigma^2}{I_{l,k}^n(t-1) + 1},$$

$$a_{l^*,k}^{n^*} = 1,$$

$$S = S \setminus \{n\}$$

end

end

Remark: At the subcarrier allocation of the first stage, we do not need to consider the interference of other fBS because no fBS decides their power allocation.

4.2.4 Noncooperative Power Allocation Game

As the subcarrier assignment for all femtocells can be decided by previous section, the noncooperative resource allocation problem turns into a noncooperative power allocation game defined as

(p.2)

$$\max \quad u(\mathbf{p}_k, \mathbf{p}_{-k}) = \sum_{n=1}^N a_{l^*,k}^{n^*} \log_2(1 + p_{kl^*,k}^{n^*}(t) g_{l^*,k}^{n^*}(t)) \quad (4.7)$$

subject to

$$p_{kl^*,k}^{n^*}(t) \geq 0 \quad \forall l, n; \quad (4.8)$$

$$\sum_{n=1}^N p_{kl^*,k}^{n^*}(t) \leq P_{fem} \quad (4.9)$$

$$p_{kl^*,k}^{n^*}(t) \leq \bar{P}_{ma}^n \quad \forall l; \quad (4.10)$$

The difference between **(p.1)** and **(p.2)** is that in **(p.2)**, we use time index to distinguish the current parameters that fBS needs to solve with last iteration parameters. For example, the GINR of fMS l in femtocell k is defined as

$$g_{l,k}^n(t) = \frac{h_{kl,k}^n}{I_{l,k}^n(t-1) + \sigma^2} = \frac{h_{kl,k}^n}{p_{ml,k}^n(t-1)h_{ml,k}^n + \sum_{i=1, i \neq k}^K p_{il,k}^n(t-1)h_{il,k}^n + \sigma^2} \quad (4.11)$$

where the interference from mBS and other fBSs is decided at the previous stage.

The solution of **(p.2)** can be derived easily via water filling, i.e., $\mathbf{p}_k = WF_k(\mathbf{p}_{-k})$, $\forall k \in K$, where the water-filling operator $WF_k(\cdot)$ on subcarrier n is defined as

$$[WF_k(\mathbf{p}_{-k})]_n = p_{l^*,k}^n = \left\{ \frac{1}{\lambda_k} - \frac{\sigma^2 + \sum_{i=1, i \neq k}^K p_{il^*,k}^n h_{il^*,k}^n}{h_{kl^*,k}^n} \right\}_0^{\bar{P}_{mac}^n}, \forall n \quad (4.12)$$

where $(x)_a^b \triangleq \max\{a, b\}$ and λ_k is such that

$$\sum_{n=1}^N p_{l^*,k}^n = P_{fem} \quad (4.13)$$

4.2.5 Randomization

Due to the occurrences of oscillation, a procedure called randomization is called for to achieve convergence. We will discuss on what condition the oscillation happens and why randomization can reduce the probability of oscillation in the next chapter. Here, we propose two randomization schemes.

► Scheme 1

Step 0: Initialize a biased coin with head probability P_c by fBSs. If this randomization is used again then skip this step.

Step 1: The fBSs start to toss coin if they meet oscillation. When tail occurs, those fBSs choose the fMS whose GINR is the second largest in the same femtocell; or remain using the same fMS with the largest GINR.

► Scheme 2

Step 0: Initialize a biased coin with head probability P_c by fBSs. If this randomization is used again then skip this step.

Step 1: The fBSs start to toss coin if they meet oscillation. When tail occurs, those fBSs do not change strategy determined in the previous iteration; or remain using the strategy decided in this iteration.



Chapter 5

Convergence and Unique NE point

We have discussed the noncooperative resource allocation game and algorithm in the previous chapter and we want to make sure whether our game can converge to a unique point. In [14][15], the authors prove that under some (sufficient) conditions on transmit powers, channels and network topology, the NE for game is unique. Since there is no reason to expect our system to be initially at the equilibrium, the concept of equilibrium has a useful meaning in practice only if one is able to find a procedure that reaches such an equilibrium from non-equilibrium states. Since we are interested in a decentralized implementation, where no signaling among different femtocells is allowed, we consider only totally distributed iterative algorithms, where each fBS acts independently of the others to optimize its own resource allocation while perceiving the other fBSs as interference. If we can meet the sufficient condition mentioned below, the NRAG can converge to the unique NE point.

5.1 Sufficient Condition for Unique NE Point

The convergence of our algorithm to a unique NE point is guaranteed under the following sufficient conditions.

Theorem: Assume that the following condition is satisfied:

$$\rho(S_{K \times K}^{max}) < 1 \quad (5.1)$$

where $S_{K \times K}^{max}$ is defined in (5.2) and $\rho(S_{K \times K}^{max})$ denotes the spectral radius of S^{max} . Then our algorithm can converges to the unique NE point of noncooperative resource allocation game for any set of feasible initial conditions and updating schedule.

$$S_{K \times K}^{max} \triangleq \begin{cases} \max_{n \in D_k \cap D_i} \frac{h_{il^*,k}^n P_i}{h_{kl^*,k}^n P_k}, & \text{if } k \neq i \\ 0, & \text{otherwise.} \end{cases} \quad (5.2)$$

$$= \begin{pmatrix} 0 & \frac{h_{2l^*,1}^n P_2}{h_{1l^*,1}^n P_1} & \cdots & \frac{h_{i-1l^*,1}^n P_{i-1}}{h_{1l^*,1}^n P_1} & \frac{h_{il^*,1}^n P_i}{h_{1l^*,1}^n P_1} \\ \frac{h_{1l^*,2}^n P_1}{h_{2l^*,2}^n P_2} & 0 & \cdots & \frac{h_{i-1l^*,2}^n P_{i-1}}{h_{2l^*,2}^n P_2} & \frac{h_{il^*,2}^n P_i}{h_{2l^*,2}^n P_2} \\ \vdots & \vdots & \ddots & \vdots & \vdots \\ \frac{h_{1l^*,i}^n P_1}{h_{il^*,i}^n P_i} & \frac{h_{2l^*,i}^n P_2}{h_{il^*,i}^n P_i} & \cdots & \frac{h_{i-1l^*,i}^n P_{i-1}}{h_{il^*,i}^n P_i} & 0 \end{pmatrix} \quad (5.3)$$

There is still another sufficient condition for unique point given by one of the two following set of conditions:

$$\sum_{i \neq k} \max_{n \in D_k \cap D_i} \frac{h_{il^*,k}^n P_i}{h_{kl^*,k}^n P_k} < 1, \forall k \in K \quad (5.4)$$

$$\sum_{k \neq i} \max_{n \in D_k \cap D_i} \frac{h_{il^*,k}^n P_i}{h_{kl^*,k}^n P_k} < 1, \forall i \in K \quad (5.5)$$

Condition (5.4) imposes a constraint on the maximum amount of interference that each receiver can tolerate. Condition (5.5) introduces an upper bound on the maximum level of interference that each transmitter is allowed to generate.

Proof: If we want to use the contraction mapping with fixed point theory, the existence of a NE for the game is guaranteed by the existence of fixed point for mapping T.

Given $WF(\mathbf{p}) = (WF_k(\mathbf{p}_{-k}))_{k \in K}$

$$\|WF(\mathbf{p}^{(1)}) - WF(\mathbf{p}^{(2)})\| = \|T(\mathbf{p}^{(1)}) - T(\mathbf{p}^{(2)})\| \leq \beta \|\mathbf{p}^{(1)} - \mathbf{p}^{(2)}\|, \forall \mathbf{p}^{(1)}, \mathbf{p}^{(2)} \in P$$

where $\|\cdot\|$ is a proper vector norm and $\beta \in [0, 1)$, where β is defined in the next page.

If the contraction mapping with $\beta \in [0, 1)$ are satisfied, then $\|S_{K \times K}^{max}\|_{\infty} < 1$.

where $\beta = \|S_{K \times K}^{max}\|_{\infty}$

$$S_{K \times K}^{max} \triangleq \begin{cases} \max_{n \in D_k \cap D_i} \frac{h_{il^*,k}^n P_i}{h_{kl^*,k}^n P_k}, & \text{if } k \neq i \\ 0, & \text{otherwise.} \end{cases} \quad (5.6)$$

where each set D_k can be shosen as any subset of $\{1, \dots, N\}$.

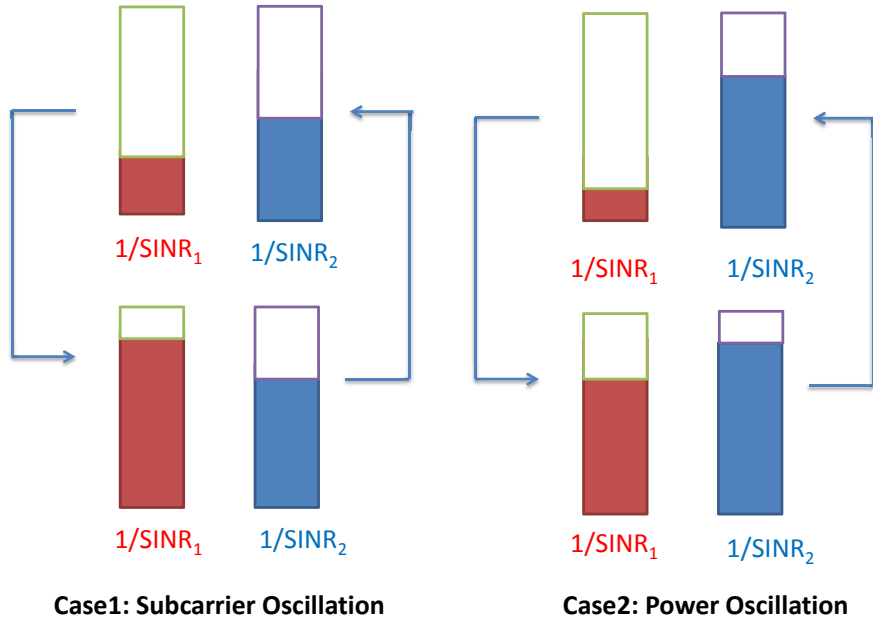


Figure 5.1: Oscillation.

5.2 Non-Convergence of Distributed Approach

5.2.1 Causes and Cases of Oscillation

Why there exists oscillation? Here, we provide two different cases that cause oscillation. The first case is that fBSs find the GINR of some subcarriers is good, so the fBSs allocate more power on these subcarriers. In some femtocell the fMS with the best GINR is selected to use the subcarrier. When other fBSs allocate more power on these subcarrier, the fMSs with best GINR may suffer more severe interference than other fMSs in the same femtocell. In the next iteration, the fMS with the best GINR in the previous iteration may become worse because of severe interference and fMS with better GINR is selected to use the subcarrier in this iteration and other femtocells also have the same situation. Those fBSs allocate lower power on this subcarrier that may reduce the interference to nearby fBSs. Thus at next iteration, the GINR of this subcarrier in

those femtocell also becomes better because the interference from other fBSs is reduced. Thus the user selection may change to the one before the previous iteration with the best GINR. The same condition iterates again and again that results in the oscillation of user selection in this subcarrier.

Another case is that at least two fBSs decide to transmit more power at the same subcarrier. But at next iteration, the GINR of this subcarrier of all fBSs decreases because of increasing interference from other fBSs and power allocated on this subcarrier become less because of worst GINR of selected fMS. But at next iteration, the interference from other fBSs decreases and the GINR of all fMSs become better than that in the previous iteration, so the fBSs allocate more power on this subcarrier with the selected fMS. The same condition repeats again and again so the game cannot converge to a stable state.

Here we show two simple cases. From Case 1 (depicted in Fig. 5.1), we first choose fMS 1 to use the subcarrier because of better GINR. But at next iteration, fMS 1 suffers severe interference from other fBS than fMS 2 that the GINR of fMS 2 is better than fMS 1 in this iteration so the fBS in this cell chooses fMS 2 to use the subcarrier. However, because other fBSs also have the same condition at this iteration, they allocate less power on this subcarrier because of worse GINR. At next iteration, because the interference from other fBSs is reduced on this subcarrier, the GINR of fMS 1 is better than fMS 2, the fBS reselect the fMS 1 to use this subcarrier. The oscillation of user selection happens again and again.

As with Case 2 (depicted in Fig. 5.1), the oscillation in power allocation process happens within two or more fBSs. At first the fMS 1 is selected with better GINR and allocated power. However, the same situation may happen in other femtocells so at next iteration the fMS1 is allocated less power because of worse GINR. At the next iteration, because the interference from other fBS is reduced, the same condition become as origin that the oscillation happens.

5.2.2 Randomization for Reducing the Probability of Oscillation

Why randomization can reduce the probability of non-convergence? The reason is that when fBSs meet the oscillation and start to use the first scheme of randomization, we use the second largest GINR to use the subcarrier. After water filling allocation, the allocated power on this subcarrier will decrease so the interference from this fBS or other fBSs may decrease. Thus the probability of Case 1 and Case 2 will be reduced. By second scheme of randomization, when the fBS does not change its strategy this iteration, then the interference from this fBS to other fBSs still remain the same. Thus the Probability of Case1 and Case 2 is also reduced and the illustration shown in Fig. 5.2.

5.2.3 Power Allocation with per Subcarrier Power Constraint

With the power upper bound, the power on all subcarriers of all femtocells are restricted. It is obvious that interference caused by every fBS to nearby femtocells can thus be reduced. In addition, the stricter the power upper bound is, the less occurrences of non-convergence happens. In the following part, we provide some explanations about this phenomenon and also use two possible cases as previous section with fBS1 and fBS2 located in a same femtocell.

Case 1 (depicted in Fig. 5.1)–the user selection oscillation. While the power upper bound employed on all fBSs, the interference level is controlled. So the user selection oscillation in Case 1 of figure1 will decrease because the interference from other fBSs is reduced and the GINR of fMS 1 is not easily worse than fMS 2. Thus oscillation of the user selection will be reduced obviously. Case 2 (depicted in Fig. 5.1)–the power allocation oscillation. While the interference from all fBS is reduced because of power upper bound, the probability of oscillation is also reduced.

There exists another explanation of reducing the probability of non-convergence with

power upper bound. When our system does not consider the power upper bound, the power allocation obviously depends on the GINR of fMSs. However, when we add power upper bound on each subcarrier, as the power on subcarrier with the best GINR reach the power upper bound, then extra power is removed from this subcarrier and reallocated to other subcarriers not satisfied the restriction of power upper bound. As the power upper bound becomes more strict, more subcarriers easily satisfy the power upper bound and more extra power is removed to reallocated on the other subcarriers. As our power upper bound become too tight, power on each subcarrier satisfies the power upper bound easily and become equal on every subcarrier. Thus the power allocation become equal power without considering the GINR of fMSs. Under this condition, the oscillation of subcarrier and power allocation will gradually disappear because the oscillation is no more dominated by the interference.

The figures with the employment of different power upper bound are shown from Fig. 5.3 to Fig. 5.4, and the power allocation will gradually become without considering GINR no matter the GINR is good or not. In Fig. 5.4, we can find that as the power upper bound is set very tight, the power on each subcarrier becomes equal power so that the power allocation no more depends on the GINR.

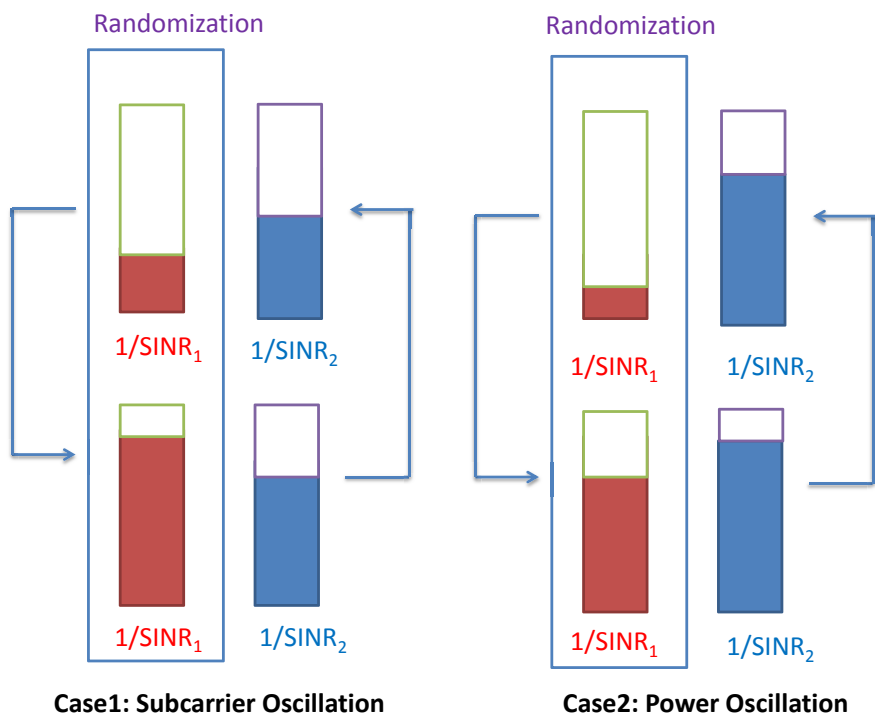


Figure 5.2: Randomization.

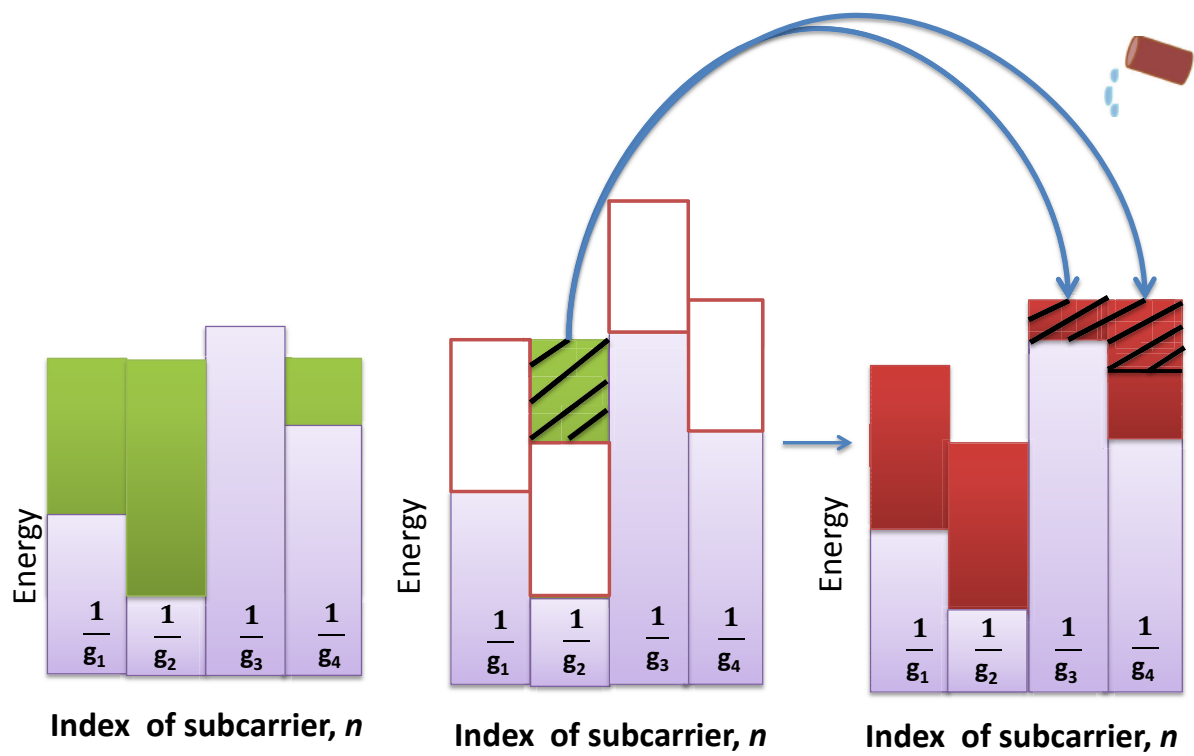


Figure 5.3: Illustration of water-filling interpretation with power upper bound.

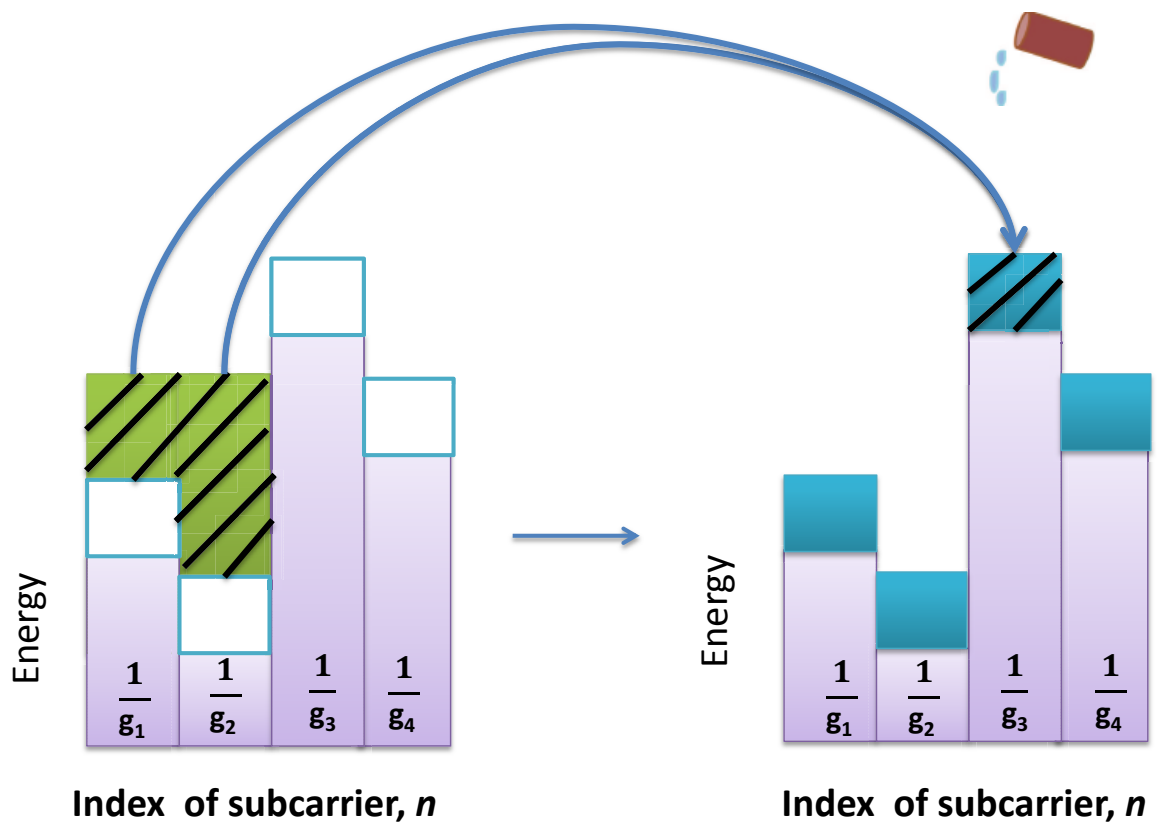
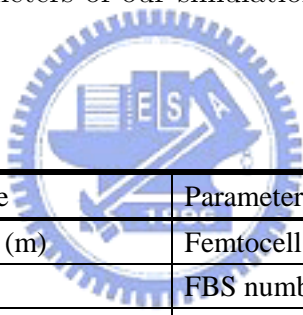


Figure 5.4: Illustration of water-filling interpretation with power upper bound.

Chapter 6

Numerical Results and Discussions

In this chapter we revisit the scenarios discussed in Chapter 2 and examine the numerical performance of our distributed algorithm applied to solve the femtocell resource allocation problems. The parameters of our simulation and path loss model are shown in table 6.1 and 6.2.



Parameter	Value	Parameter	Value
Macrocell radius	1732 (m)	Femtocell radius	10 (m)
mBS number	1	FBS number	4
mMS number	16	FMS number each femtocell	2
Macrocell total power	43 dBm (20 Watt)	Femtocell total power	23dBm (200mW)
System bandwidth	10 MHz	Number of subcarriers	128
Subcarrier bandwidth	78.125 KHz	Noise power spectrum density	-174dBm/Hz
Noise figure of macrocell	5dB	Noise figure of femtocell	8dB

Table 6.1: Simulation parameters.

Path loss models for urban (dense apartment) deployment	
Cases	Path Loss (dB)
fBS k to its fMS I_k	PL (dB) = $38.46 + 20 \log_{10}R$
fBS k to fMS I_i in other fBS i	PL (dB) = $\max(15.3 + 37.6\log_{10}R, 38.46 + 20\log_{10}R) + n_{ki} * L_{ow}$
fBS k to mMS j	PL (dB) = $15.3 + 37.6\log_{10}R + n_{kj} * L_{ow}$
mBS to mMS j	PL (dB) = $15.3 + 37.6\log_{10}R$
mBS to fMS I_k in fBS K	PL (dB) = $15.3 + 37.6\log_{10}R + n_{mk} * L_{ow}$

R is the Tx-Rx separation(R in m)
 L_{ow} is the penetration loss of an outdoor wall, which is 10dB
 n_{ki} = the number of wall between fBS k to fMS I_i in other fBS i
 n_{kj} = the number of wall between fBS k to mMS j
 n_{mk} = the number of wall between mBS to fMS I_k in fBS K

Table 6.2: Pathloss model.

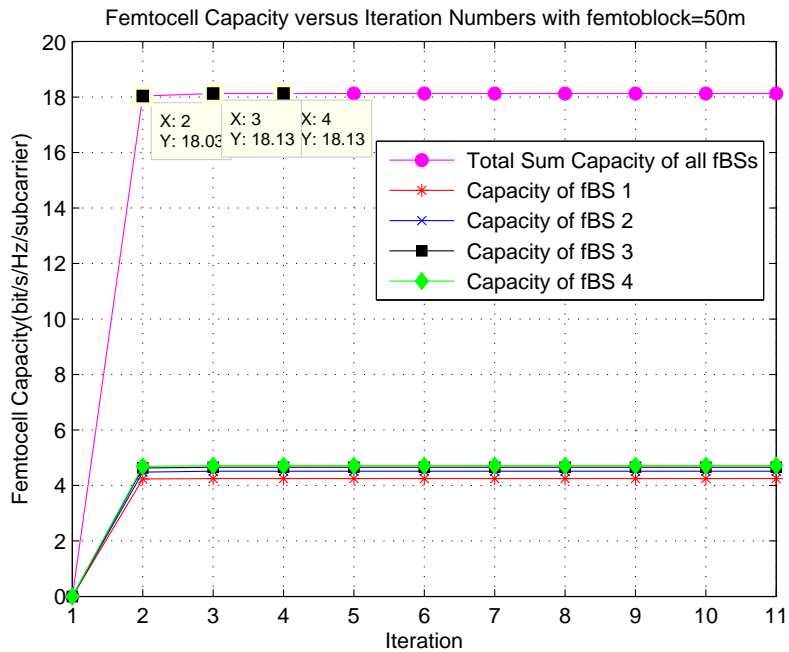


Figure 6.1: Convergence Case of Noncooperative Game.

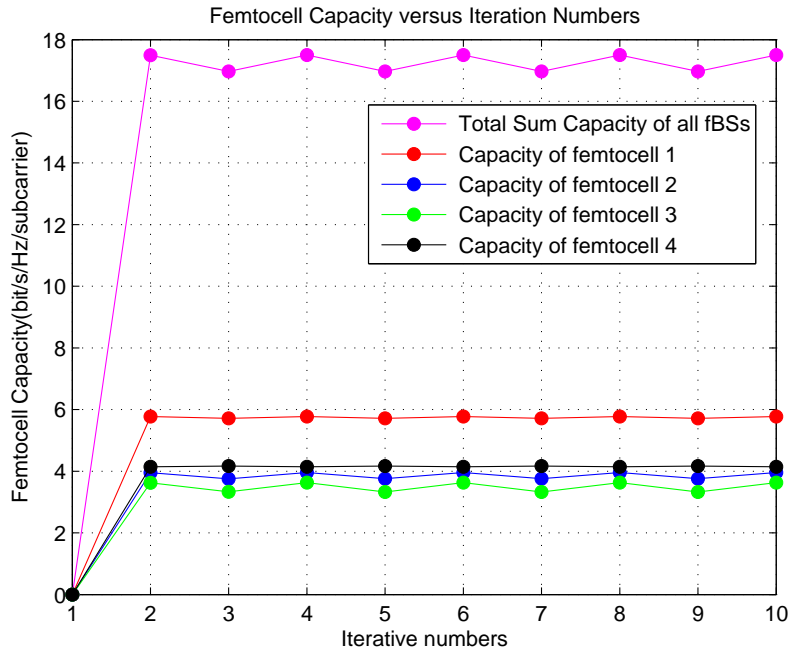


Figure 6.2: Nonconvergence Case of Noncooperative Game.

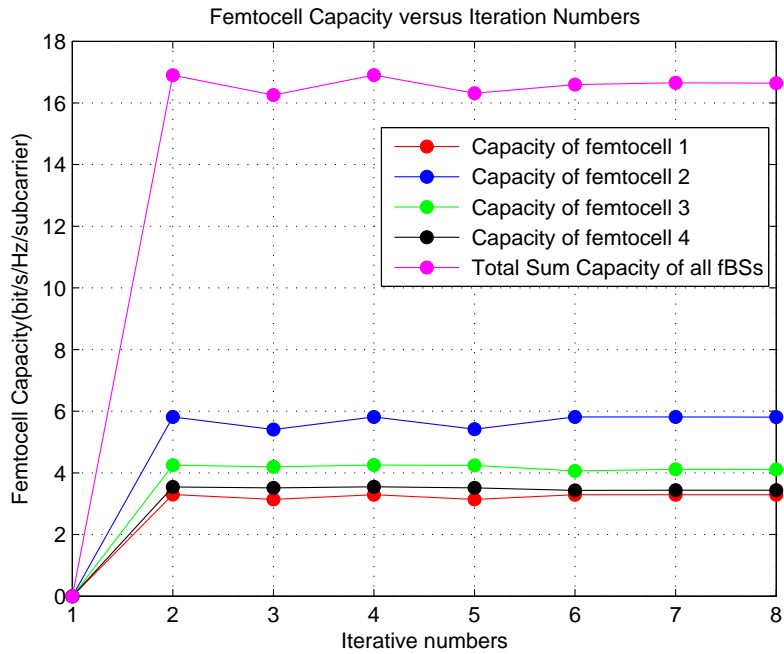


Figure 6.3: Convergence result by using Variance Reduction

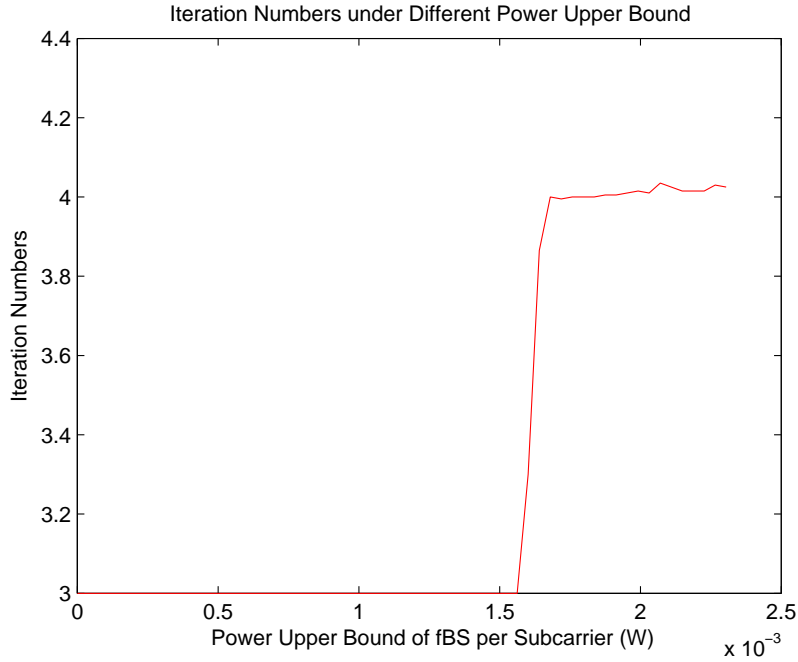


Figure 6.4: Iteration number with different power upper bound.

Fig. 6.1 shows the capacity tendency of normal case. But in Fig. 6.2, we find sometimes the non-convergence case may happen with our distributed algorithm. However, with several variation reduction approaches, the non-convergence case can be reduced obviously and shown in Fig. 6.3.

From Fig. 6.4, while the power upper bound of our system is tight, the allocated power on all subcarrier becomes equal that is discussed in chapter 5. We find that as the power upper bound is under 1.5×10^{-3} , the power allocation on all subcarriers is equal. At the third iteration, all fBSs do not change the power allocation and the interference from other fBSs remains the same so fBSs finish the game. As the power upper bound is above 1.5×10^{-3} , the power allocation varies on different subcarriers and the interference from different fBSs may affect the power allocation of all fBSs that leads to increasing iteration numbers of noncooperative game.

If our fBSs find oscillation and start to use randomization, the requirement of iteration numbers from using randomization to convergence is shown in Fig. 6.5 and Fig. 6.6.

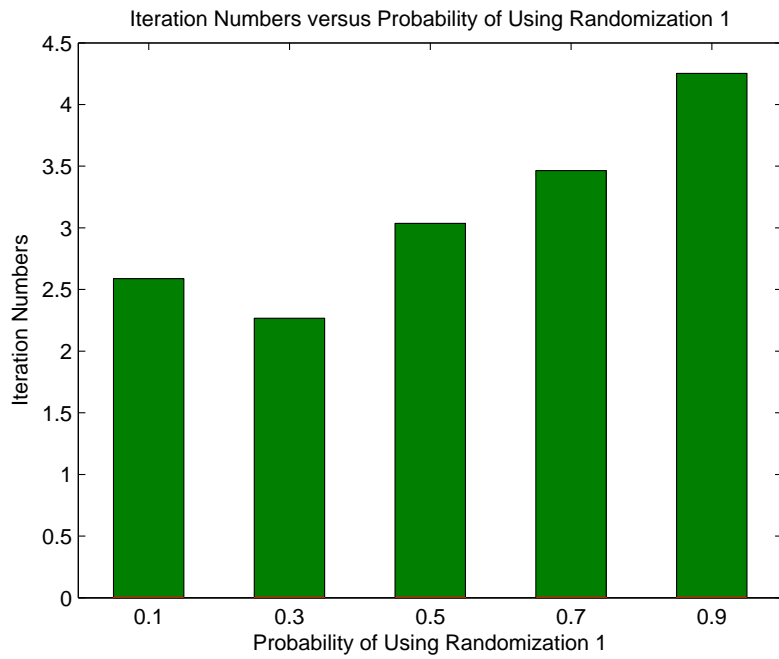


Figure 6.5: Iteration numbers versus probability of using randomization 1.

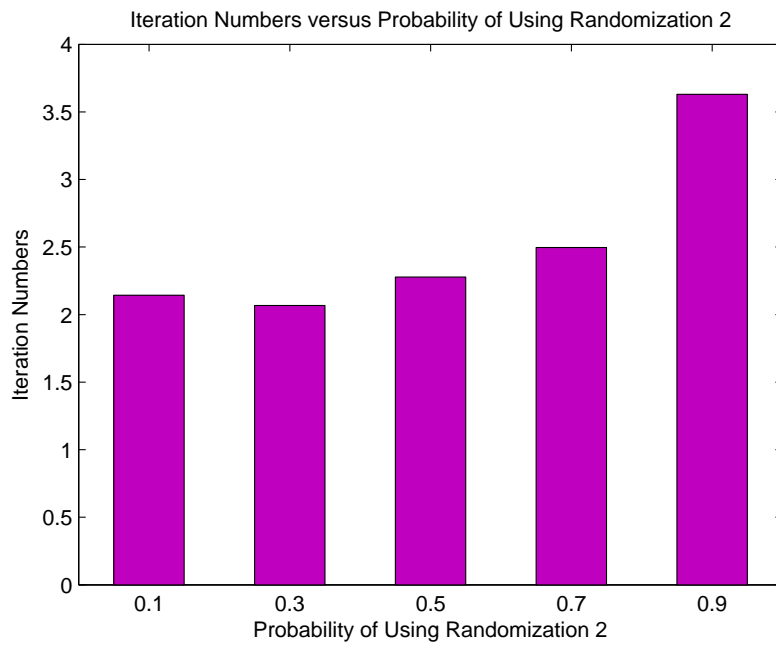


Figure 6.6: Iteration numbers versus probability of using randomization 2.

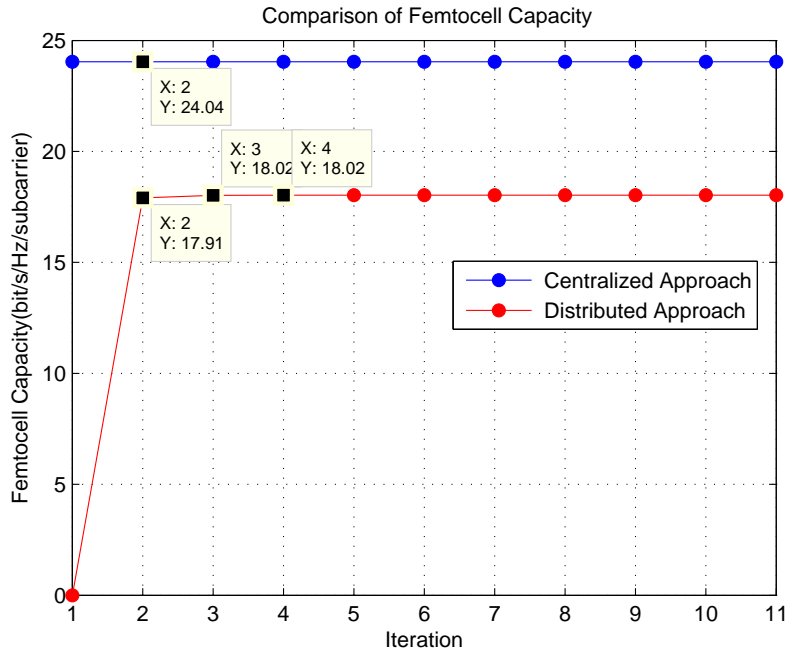


Figure 6.7: Comparison of Femtocell Capacity.

From the illustrations we can realize that if the probability of using randomization is few, the oscillation still happens that causes more iteration numbers to converge. In other words, the iteration numbers can be reduced if the fBSs use randomization frequently.

In Fig. 6.7, we want to compare the femtocell capacity with two different approaches: one is centralized algorithm, the other is distributed method. The centralized approach is exhausted research that requires all combinations of user selection with jointly iterative power allocation solved by convex-optimization soft cvx. As shown in the illustration, the centralized approach can gain 25% bandwidth efficiency than distributed method. Though centralized approach can achieve higher bandwidth efficiency, high computational complexity and knowing all information are impractical in the practical system.

Finally, we want to investigate the femtocell capacity with power upper bound imposed on the fBSs. From Fig. 6.8, we can find the femtocell capacity near the mBS is lower than that far from mBS because the fBSs near mBS suffer more macrocell interference. However, the femtocell capacity at distance 1500 is also lower than that at

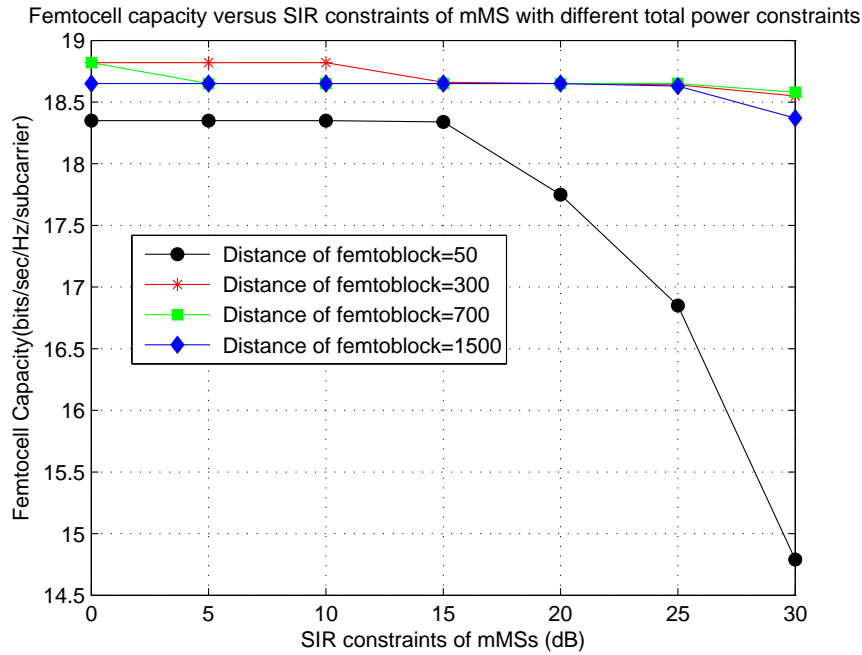


Figure 6.8: Femtocell capacity versus SIR constraints of mMSS with different power constraints.

distance 300 and 700. The reason is that the fBSs at distance 1500 have been imposed strict power upper bound to protect the QoS of mMSSs and are allocated equal power on all subcarriers that cause less capacity than water filling power allocation. As the requirements of mMSSs' QoS increase, all fBSs are imposed more strict power upper bound on all subcarriers. The fBSs at location 50 suffer not only noise power but also severe interference from macrocell, so the femtocell capacity decreases rapidly. The femtocell capacity at different distance does not decrease rapidly because the interference is mainly dominated from other fBSs and larger than power noise. Only when the power upper bound is too tight that the noise power also affects the SINR of fBSs, the femtocell capacity decreases as the requirement of mMSSs' SIR achieves 30 dB.

Chapter 7

Conclusion

Femtocell network can effectively enhance indoor coverage and provide high data rate for indoor users due to the short distance between fBS and mMSSs. However, how to manage interference between macrocell and femtocell network is a critical issue. One of our goals in this thesis is to find a solution of interference management problem without information about channel conditions and locations of mMSSs. Then resolve the downlink resource allocation problem for femtocell by distributed approach in the femtocell and macrocell overlay network.

First, we propose average outage probability constraint for fBS as a criterion to protect the QoS of mMSSs. However, without assuming perfect information about channel conditions and locations of mMSSs, calculating the average probability constraint is a difficult task for fBSs. Thus, we provide the closed form outage probability with fixed locations of mMSSs and fBSs in chapter 3. After finding the outage probability of fixed locations of fBSs and mMSSs, we can find the outage probability with two different schemes: one is distributed locations of fBSs, the other is fBSs fixed in femto block. At last, we can find the maximum acceptable power of fBSs from the average outage probability constraint.

The distributed approach is proposed to solve the resource allocation problem in an OFDMA-based femtocell overlay network. Regarding the distributed RA as a non-

cooperative game, the sufficient condition for existence of a Nash equilibrium point is provided. On the other hand, several variation reduction remedies are provided to reduce the non-convergence probability of resource allocation. We also try to interpret the convergence of our algorithm and the remedies. Finally, the simulation shows the bandwidth efficiency of femtocell system is influenced by power upper bound and mutual interference of fBSs.



Bibliography

- [1] Femto forum. <http://www.femtoforum.org>.
- [2] Y. Bai, J. Zhou, L. Liu, L. Chen, and H. Otsuka, "Resource coordination and interference mitigation between macrocell and femtocell," in *Proc. PIMRC*, Tokyo, Japan, pp.1401-1405, Sept. 2009
- [3] D. Lopez-Perez, A. Ladanyi, A. Juttner, and J. Zhang, "OFDMA femtocells: a self-organizing approach for frequency assignment," in *Proc. PIMRC*, Tokyo, Japan, pp.2202-2207, Sept. 2009
- [4] K. Han, Y. Choi, D. Kim, M. Na, S. Choi, and K.Han, "Optimization of femto-cell network configuration under interference constraints," in *Proc. WIOPT*, Seoul, Korea, pp.1-7, June 2009
- [5] V. Chandrasekhar, and J. G. Andrews, "Uplink capacity and interference avoidance for two-tier femtocell networks," *IEEE Trans. Commun.*, vol.8, pp.3498-3509, July 2009
- [6] M. Haenggi, J.G. Andrews, F. Baccelli, O. Dousse and M. Franceschetti, "Stochastic geometry and random graphs for the analysis and design of wireless networks," *IEEE J. Sel. Areas Comm.*, vol.27, pp.1029-1046, Sept. 2009
- [7] Y. Zhang, C. Zhang, J. Cosmas, K. -K. Loo, T. Owens, R. Di Bari, Y. Lostanlen, and M. Bard, "Analysis of DVB-H network coverage with the application of transmit diversity," *IEEE Trans. Broadcast.*, vol. 53, pp.578-589, Sept. 2008

- [8] Hojoong Kwon, and Byeong Gi Lee, "Distributed Resource Allocation through Non-cooperative Game Approach in Multi-cell OFDMA Systems," *in Proc. IEEE ICC*, June 2006, pp. 4345V4350.
- [9] Z. Liang, Y. H. Chew, and C. C. Ko, "On the Modeling of a Noncooperative Multicell OFDMA Resource Allocation Game with Integer Bit-Loading," *Globecom* 2009.
- [10] Gesualdo Scutari, Daniel P. Palomar, and Sergio Barbarossa, "Asynchronous Iterative Water-Filling for Gaussian Frequency-Selective Interference Channels," *IEEE TRANSACTIONS ON INFORMATION THEORY*, VOL. 54, NO. 7, JULY 2008
- [11] Fan Wang, Marwan Krunz, and Shuguang Cui, "Price-Based Spectrum Management in Cognitive Radio Networks," *IEEE JOURNAL OF SELECTED TOPICS IN SIGNAL PROCESSING*, VOL. 2, NO. 1, FEBRUARY 2008.
- [12] R. Cendrillon, W. Yu, M. Moonen, J. Verlinden, and T. Bostoen, "Optimal multi-user spectrum management for digital subscriber lines," *IEEE Trans. Commun.*, vol. 50, pp. 291V303, Feb. 2006.
- [13] Ho Van Khuong, and Hyung-Yun Kong, "General Expression for pdf of a Sum of Independent Exponential Random Variables," *Communications Letters, IEEE*, Volume 10, Issue 3, March 2006 Page(s):159 - 161.
- [14] G. Scutari, D. P. Palomar, and S. Barbarossa, "Optimal linear precoding strategies for non-cooperative systems based on game theory- Part I: Nash equilibria," *IEEE Trans. Signal Process*, vol. 56, no. 3, Mar. 2008.
- [15] G. Scutari and D. P. P. Barbarossa, "Optimal linear precoding strategies for wide-band non-cooperative systems based on game theory-part II: Algorithms," *IEEE Trans. Signal Process.*, vol. 56, no. 3, pp. 1250V1267, Mar. 2008.